Potential of a Water Balance Model with High Temporal Resolution for the Distributed Modelling of Ice- and Snowmelt Processes at High Elevated Sites

GERNOT KOBOLTSCHNIG[1], HUBERT HOLZMANN[1],
WOLFGANG SCHOENER[2], AND MASSIMILIANO ZAPPA[3]

ABSTRACT

The potential of the distributed hydrological water balance model PREVAH at the small, highly glacierized catchment area of Goldbergkees in the Austrian Alps has been investigated. The model is driven by meteorological data from the observatory at Hoher Sonnblick, situated at the highest point of the catchment area. A dense network of field observations as additional input and validation data has been applied. In the final setting PREVAH has been run in an hourly time step based on 722 hydrological response units covering the catchment area. Both snow- and icemelt have been simulated by means of an advanced air temperature-index based approach taking potential direct solar radiation into account. A multi-validation approach using discharge hydrographs, measured snow water equivalent data (SWE), snow cover patterns derived from satellite data, and glacier mass balance investigations have been applied to validate the water balance of the hydrological year of 2004/2005. The comparison of modelled SWE with spatially dense SWE measurements at four different dates within the period May to July 2005 shows quite good accordance for both individual elevation bands and the entire catchment. The period of 2003/2004 has been used for cross-validating the model for discharge-hydrograph and ice melt. Icemelt and maximum snow accumulation have been validated against glacier mass balance measurements. The individual components contributing to runoff such as rainfall, snow- and icemelt have been separated for the hydrological year 2004/05 to estimate their fraction to total discharge which is 3.8% for rain, 86.8% for snow, and 9.4% for ice respectively. Finally recommendations are given for a possible improvement of hydrologic models considering snow- and icemelt at high elevated sites.

Keywords: glacier melt; snowmelt; alpine hydrology; water balance of high elevated sites; SWE investigation

INTRODUCTION

According to the location, elevation and topography the contribution to runoff from glacier melt, snowmelt and rainfall at glacierized, alpine watersheds varies strongly depending on climate

[1] University of Natural Resources and Applied Life Sciences (BOKU), Muthgasse 18, A-1190 Vienna, Austria. E-mail: gernot.koboltschnig@boku.ac.at
[2] Central Institute of Meteorology and Geodynamics (ZAMG), Hohewarte 38, A-1190 Vienna, Austria
[3] Swiss Federal Institute for Forest, Snow and Landscape Research (WSL), Zürcherstrasse 111, CH-8903 Birmensdorf, Switzerland

conditions (Singh and Bengtsson, 2005). For calculating the water balance of glacierized watersheds, meteorological data have to be obtained for the entire hydrological year to fully cover the process of snow accumulation during winter period as well as the snow- and icemelt during summer period. Icemelt depends on snow depletion of the glacier and the area of bare ice exposed to melt. Consequently, the knowledge of the distributed snow accumulation is of high importance to simulate the snow line retreat at the catchment area (Blöschl et al., 1991). The numerical modelling of all of the components contributing to runoff and their superposition requires tools for the assessment of spatially interpolated meteorological variables, as well as for the treatment of distributed geographical variables (Kirnbauer et al., 1994; Gurtz et al., 2003). Due to the complexity of different hydrological processes at high elevated sites a multi-validation of simulation results is needed (e.g. Günter et al., 1999). Verbunt et al. (2003) recommended using discharge hydrographs, water balance elements, snow water equivalent data or soil moisture values. High elevated sites with sparse hydro-meteorological observations make model assumptions e.g. temperature-index models using wide available and easy to spatially interpolate air temperature data necessary. The use of temperature-index models already has a long history. Such a relation was first applied for an Alpine glacier by Finsterwalder and Schunk (1887). Hock (1999) and Pellicciotti et al. (2005) adapted the classical degree-day method for glacierized areas linking air temperature to global radiation respectively potential clear-sky direct solar radiation to improve the diurnal cycles of melt.

The physical basis of temperature-based melt-index methods is demonstrated by Ohmura (2002). The paper concluded that the longwave atmospheric radiation is the most dominant heat source, and the majority of the atmospheric radiation received at the surface comes from the near-surface layer of the atmosphere. Hence, there is a good, physical based relation between air temperature and melt.

Many studies have been presented for the simulation of snowmelt, icemelt or both for meso-scale basins with physically based (Cline et al., 1998; Marks et al, 1999; Lehning et al., 2006) and conceptual approaches (Schaefli et al., 2005; Klok et al. 2001; Verbunt et al. 2003), but only few studies tested the applicability of such models for very small basins (Arnold et al., 1996 & 1998). Zappa et al. (2003) introduced a study comparing different temperature-index models and an energy balance model for the snowmelt modelling of an alpine catchment. They showed that the improved temperature-index model (according to Hock, 1999) performed better than the energy balance approach implemented in PREVAH.

Thus, the main goal of this study has been to assess the potential of a distributed hydrological modelling in a highly glacierized, small, and high elevated basin. For this we simulated the water balance for the hydrological year 2004/2005 of the Goldbergkees watershed (Austria) with the conceptual distributed hydrological model PREVAH (Precipitation–Runoff–Evapotranspiration–HRU model, Gurtz et al., 1999). For validation we compared the computed results with maps of the snow water equivalent derived from detailed field campaigns (similar to Elder et al. 1998), with a remotely sensed map of the snow distribution (as e.g. Cline et al., 1998; Blöschl et al., 2002), with observed data of the glacier mass balance (as e.g. Schaefli et al., 2005) and with runoff data gauged during the summer and fall at the basin outlet.

STUDY REGION

Glacier Goldbergkees is situated directly beneath the Hoher Sonnblick observatory (3106 m a.s.l., 47°03’16” N, 12°57’25” E) in the central part of the Austrian Alps (Figure 1). Hoher Sonnblick is the oldest and highest, permanently staffed observatory in the Alps above 3000 m a.s.l.. Meteorological observations at the observatory are available back to 1886, detailed mass balance measurements at the nearby glaciers started in 1983 (Auer et al., 2002), and detailed hydrological investigations are carried out since 2002. Hence a wide range of hydrological, meteorological and glaciological observations are available for detailed melt runoff and water balance modelling. The Goldbergkees watershed has an area of about 2.72 km² with a about 52 % glacierized (1.43 km² computed for 2003). Elevations ranges between 2350 and 3106 m a.s.l.. The catchment area is well defined by an automatic discharge gauging station at about 250 meters distance downstream the glacier tongue situated at the outlet of a lake (Figure 1). The solid rock river bed and nearly laminar flow guarantees reliable runoff gauging. The area is structured into three major topographical sections: The upper part comprises south and southeast facing slopes, the middle part faces east and northeast, and the lower part comprises the tongue of the glacier which faces north and north east. All parts of the catchment are above the timber line. The dominant land cover is rock (central alpine gneiss), gravel and ice (unpublished data from Koboltschnig et al., 2006). The mean air temperature at Sonnblick observatory is about –5.7°C. The annual precipitation at Sonnblick observatory averages about 2680 mm, with 89% as snow (climate normals 1961–1990, Auer et al., 2002).

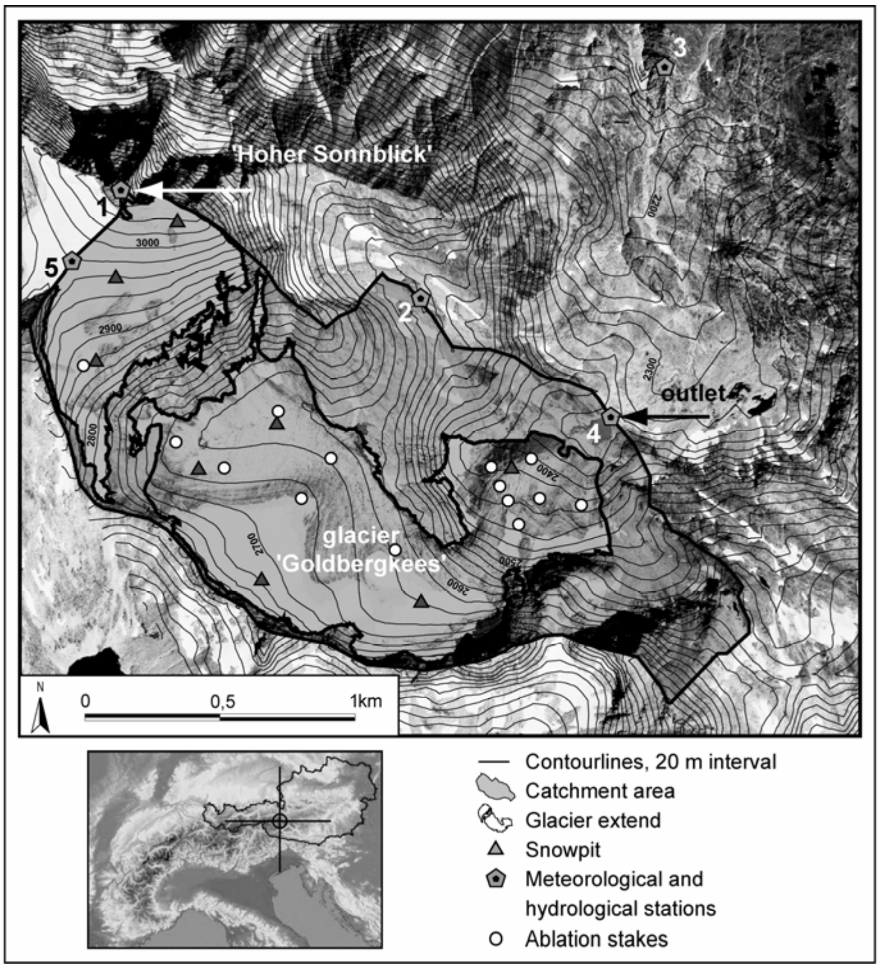

Figure 1. Catchment area of Goldbergkees. Numbers from 1 to 5 indicate hydro-meteorological stations: 1 observatory at the top Hoher Sonnblick; 2 air temperature station; 3 air temperature station; 4 discharge gauge, air temperature station, and temporary tipping bucket; 5 automatic ultra sonic snow depth measurement

METHODS

Field investigations and meteorological network

Hourly data of precipitation, air temperature, moisture, wind speed, sunshine duration and global radiation were taken from the observatory at the top of Hoher Sonnblick (Figure 1, Nr. 1).

Precipitation and air temperature data observed at the observatory are shown in Figure 8 (e and f). Three additional air temperature stations were installed during 2005 melt season in and next to the catchment area (Figure 1, Nr. 2, 3 and 4). A temporary tipping bucket, for liquid precipitation measurements only, was installed at the catchment outlet (Figure 1, Nr. 4). The tipping bucket was fixed together with the temperature station and the data logger of the discharge gauge. Water levels could only be recorded between July and October at a natural cross section of a lake outlet. To prevent damage the instrumentation has to be removed during winter period. The rating curves were calculated for every melt season separately due to the changes of the hydraulic conditions. Snow depths have been measured automatically in a daily interval at about hundred meters of elevation beneath the observatory (see Figure 1, Nr. 5). Starting in May 2005 four field campaigns for mapping the SWE (snow water equivalent) of the catchment area were performed in monthly steps. Aluminium probes were used to measure the snow depth at about 60 to 140 points irregularly distributed over the entire catchment area. The snow density has been measured at two snow pits following the instructions of Kaser et al. (2003). During the earliest campaign in May eight pits have been dug with regard to the higher variability of the snow layers at that time (Figure 1, grey triangles). From this very detailed data set we interpolated distributed maps of SWE using a spline method to generate 10 m grids of snow depth. Additional sampling points at areas with no snow cover have been set to ensure better interpolation results at border areas. The measured snow density data have been interpolated using inverse distance weighting technique. Finally, SWE were computed from spatialized snow depth and snow density. Snow free areas were mapped in field using GPS. The maps of snow free areas have been overlaid to generate the final depletion maps. This unique set of SWE grid has been available for visual and quantitative comparison with the computation of the hydrological model (Figure 2).

As a standard program of the mass balance measurements following the glaciological method (Hoinkes, 1970; Østrem and Brugman, 1991; Kaser et al., 2003) the ice ablation have been measured using ablation stakes, which have been drilled into the bare ice of the glacier. Using 17 ablation stakes distributed over the entire ablation area of glacier Goldbergkees the net ablation of the glacier has been calculated (Hynek and Schöner, 2004).

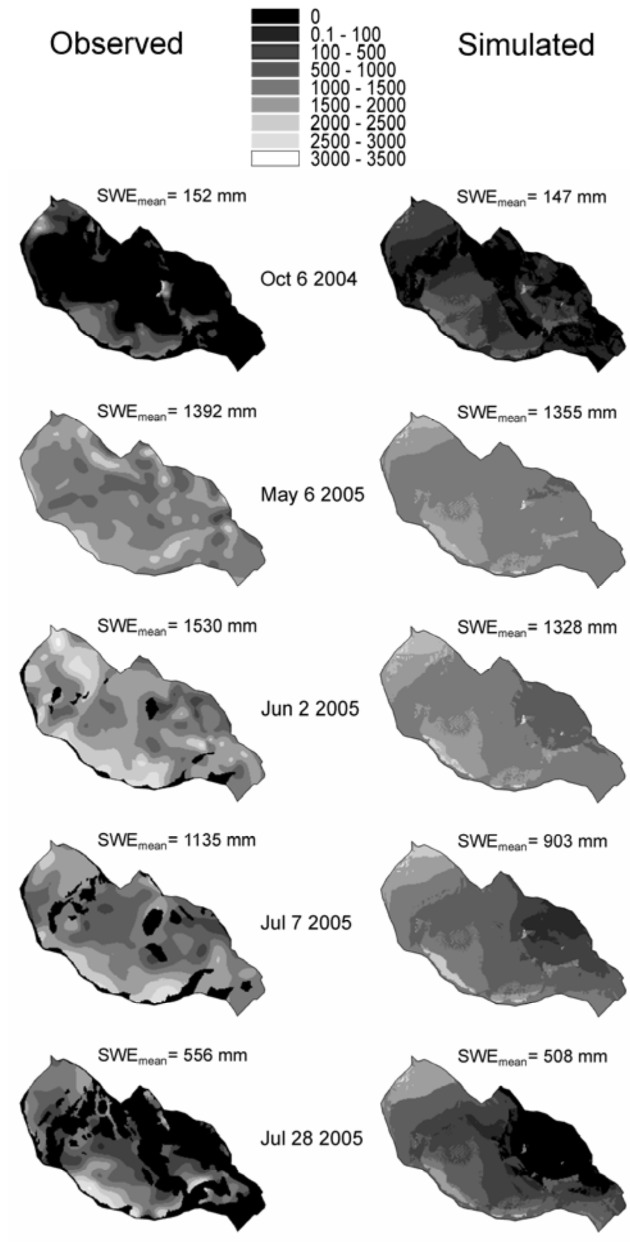

Figure 2. Simulated vs. observed distributed SWE data for different dates in 2004 and 2005. Black areas indicate snow free areas. Mentioned values of SWE_{mean} are distributed SWE values averaged over the catchment area (mm)

The hydrological model PREVAH

The spatially distributed hydrological model PREVAH (Precipitation–Runoff–Evapotranspiration–HRU model, Gurtz et al., 1999) has been used to simulate the processes contributing to runoff. PREVAH has already been used at glacierized sites at different spatial resolution (Badoux, 1999; Gurtz et al., 2003; Zappa et al., 2003; Zappa et al., 2000). The catchment area is subdivided into HRU's (hydrological response units, Ross et al., 1979) based on DEM and land use data. For every HRU the hydrological response to the meteorological input is simulated using a typical storage cascade approach. The runoff contributions of all units are added to provide the total discharge at the outlet of the entire catchment. Due to the small size of the catchment and steep slopes no routing between the spatial units and the river outlet is carried out.

The runoff delay caused by the different glacial reservoirs is managed by the main model storages for the melt simulations. This are the snow-, ice- and firn storage, parameterized using the storage coefficient and the translation time (Badoux, 1999). PREVAH uses different approaches for the snow and icemelt simulations. For this study the radiation based temperature-index approach of Hock (1999) has been applied:

$$M = \begin{cases} \frac{1}{n}(MF_{snow\,/\,ice} + a_{snow\,/\,ice} \cdot I) \cdot T & : \quad T > 0 \\ 0 & : \quad T \leq 0 \end{cases} \tag{1}$$

where M is the calculated melt rate (mm h^{-1}), $MF_{snow\,/\,ice}$ is the melt factor for snow respectively ice (mm d^{-1} K^{-1}), $a_{snow\,/\,ice}$ is the radiation melt factor for snow respectively ice, I is the potential clear-sky direct solar radiation at ice or snow surface (W m^{-2}), T is the air temperature (°C) and n is the number of time-steps per day, in this case 24 hours. The melt factors for snow and ice are empirical coefficients and I is a calculated value following Hock (1999).

Only air temperature is needed as input to the model, radiation is calculated as the site adjusted potential direct radiation for every HRU, considering exposition and slope. This approach has shown the best results in the comparative study of Zappa et al. (2003), where the performance of an energy balance model and three degree-day-factor models have been investigated for a meso-scale basin.

For the calculation of the snow accumulation, the simulation of the surface runoff, the calculation of snow- and icemelt, and the calculation of the evapotranspiration the following input to the PREVAH model is required: air temperature, precipitation, water vapour pressure, global radiation, wind speed and sunshine duration.

Model application at Goldbergkees watershed

As a major source for the description of the topography to the modelling system a DEM of 10 m resolution (Auer et al., 2002), covering the entire catchment area, has been applied. Such high resolution is required to account for the small scale variability of the investigated processes for such a small basin. The separation into HRU's has been realized using two land use classes (glacier and rock), 50 m elevation bands (16 classes), nine aspect classes and six slope classes. Thus 722 HRU's and 197 meteorological units (MU) were generated. MU are the spatial units covering the watershed for which the meteorological data have been interpolated based on hourly data from available stations (Figure 1, stations 1, 2, 3, and 4). Because elevation and exposition are the main factors governing climatological and meteorological variability in such areas, raster elements in the same elevation band and showing similar aspect belong to the same MU. The PREVAH model has been run in an hourly time step. For the interpolation of the meteorological input an inverse distance weighting and altitude-dependent regression approach has been used (Klok et al. 2001). Precipitation has been permanently observed at the observatory and temporary at the catchment outlet (Figure 1, stations 1 and 4). For a better weighting two additional virtual stations at the sites of the stations 2 and 3 (Figure 1) have been applied, where monthly measured precipitation sums have been available. The laps rate for the air temperature has been set to 0.65°K/100 m. This value has been estimated using long term air temperature measurements of two stations in the area. The air temperature input for the melt modelling is taken from 3 stations outside the glacier, which is proposed by Lang and Braun (1990).

The simulation of one entire hydrological year with PREVAH, producing tables of hourly runoff and storage output, and daily maps of SWE takes less than 3 minutes computation time using a standard PC. We proceeded therefore with manual tuning of the parameters governing the processes of snow accumulation, snowmelt, icemelt and runoff generation (Zappa et al., 2003; Gurtz et al., 2003) for the hydrological year 2004/2005, where we have additional observations on snow cover and SWE for multi-criteria verification. The verification for the discharge simulation has been carried out by the analysis of the model performance for the hydrological year 2003/2004.

Calibration procedure

First step: Due to the extreme climate conditions during 2003 melt season the catchment area of Goldbergkees glacier was nearly snow free. Hence it has been possible to calibrate the melt parameters for icemelt separated from other processes. Therefore the observed and simulated discharge hydrographs have been compared;

Second step: The model has been initialized using spatially distributed SWE data at the time of the maximum snow accumulation (begin of May). Thus the degree day factor for snowmelt has been calibrated comparing the daily results of the internal snow storage with the in field observed spatially distributed SWE data at different points in time;

Third step: The model has been initialized using spatially distributed SWE data at the beginning of the accumulation period (equal to the beginning of the hydrological year in the northern hemisphere at the beginning of October). For this reason the solid precipitation has been corrected by plus 18 % more precipitation following Sevruk (1986). The snow accumulation of the PREVAH model has been compared with the in field observed spatially distributed SWE data at the time of the maximum accumulation;

Fourth step: Fine tuning of the melt parameters and adaptation of the storage parameters comparing observed and simulated hydrographs. The storage time for snow- and icemelt are calibrated for the Goldbergkees catchment adducting the recession curves of the observed hydrograph, which result when summer snowfalls reduce ablation by raising albedo (Collins, 1982). Three events of this kind have been observed at 2005 melt season (see Figure 4). For the determination of the translation time of snow- and icemelt the diurnal maximums of the simulated runoff have been fitted to the observed hydrograph.

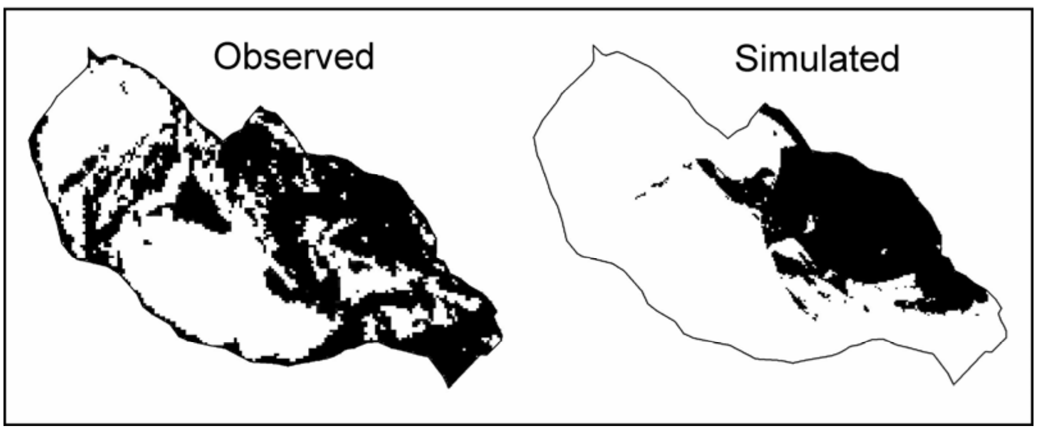

Figure 4. Simulated vs. observed snow cover pattern at 29 July 2005. The observed image is generated by a classification of an ASTER image. Black coloured areas indicate snow free areas, white areas are still snow covered.

Verification procedure

First step: the distributed SWE simulation has been verified at 4 dates of the 2004/2005 period;

Second step: the simulation of the snow patterns has been verified with satellite data from ASTER;

Third step: the skill of the runoff simulation has been independently verified without further adjustment of the calibrated parameters by comparisons with the hydrological year 2003/2004;

Fourth step: observed data on glacier ablation for both 2003/2004 and 2004/2005 have been compared with the simulated ice ablation.

Main model settings

For simulating the hydrological year of 2004/2005 the calibrated model has been initialized at the beginning of October 2004 by in field observed SWE data. The main calibrated parameters of the model are shown in Table 1 in comparison to similar studies (Pellicciotti et al., 2005; Hock, 1999; Zappa et al., 2003). The melt factors presented in this paper are of the same size as the compared values. The degree-day-factor for ice is slightly higher, which could be explained by the dark ice surface and therefore quite low albedo of Goldbergkees glacier. The snowmelt model is parameterized by the radiation melt factor and the maximum and the minimum temperature dependent melt factors, which define the maximum at 21st of June and the minimum at 21st of December of a sinus shaped function. The temperature dependent melt factor for ice is constant in time.

Table 1. Comparison of the model parameters calibrated at Goldbergkees watershed and the parameters of the studies of Pellicciotti et al. (2005), Hock (1999) and Zappa et al. (2003)

Parameter	Cal. Value	Zappa	Hock	Pellicciotti	Unit
Threshold temperature for snowmelt	0	0	0	1	[°C]
Max. degree day factor	3.2	–	–	–	[mm d^{-1} K^{-1}]
Min. degree day factor	1	–	–	–	[mm d^{-1} K^{-1}]
Degree day factor	–	0.8	1.8	1.97	[mm d^{-1} K^{-1}]
Radiation melt factor for snow	0.00015	0.00027	0.0008	0.00052	[mm W^{-1} m^2 K^{-1} h^{-1}]
Temperature melt factor for ice	2.15	–	1.8	1.97	[mm d^{-1} K^{-1}]
Radiation melt factor for ice	0.0003	–	0.0006	0.00106	[mm W^{-1} m^2 K^{-1} h^{-1}]
Storage time for snowmelt	25	–	–	–	[h]
Storage time for icemelt	2	–	–	–	[h]
Translation time for snowmelt	3	–	–	–	[h]
Translation time for icemelt	2	–	–	–	[h]

RESULTS AND DISCUSSION

Distributed snow-water-equivalent (SWE)

The PREVAH model makes a daily output of the distributed SWE storage possible. Thus the validation using observed SWE data is an additional alternative. Figure 2 shows the validation of the SWE for four different points in time starting with the initial SWE model settings of 6 October 2004. The simulated plot for this date shows the mean value of the SWE storage at the end of the first simulated day described for the internal distribution of the meteorological units. Through this semi-distributed approach some information on spatial distribution is lost. The simulated and observed maximum snow accumulation at 6 May 2005 are in a very good agreement. At 2 June 2005 the simulation shows a little smaller SWE storage than the month before but the observed SWE seems to show an overestimation through the field measurement. There is no possibility to explain the high accumulation by observed precipitation data. At 7 July 2005 still a slightly overestimation is seen. The last observation at 28 July 2005 shows a good accordance of the simulated SWE, averaged over the catchment area. The simulated distribution of snow left in the catchment strongly depends on the distribution of precipitation, whereas the in field observed distribution of snow depends on precipitation gradients, snow redistribution by wind and vertical drift of snow induced by avalanches (Hartmann et al., 1999; Blöschl et al., 1991).

The spatial analysis of the distributed observed and simulated SWE maps is shown in Figure 3. The catchment area has been divided into 8 100 m elevation bands starting at 2300 m a.s.l.. There is a very good agreement between observation and simulation at 6 May 2005 at the elevation bands between 2600 and 2900 m (Figure 3a). The upper bands show an overestimation and the lower bands an underestimation of the simulation. This result is due to the snow redistribution from the upper to the lower parts, induced by wind or avalanches. The problem of too high snow accumulation measured at 2 June 2005 can be seen in Figure 3b, where the simulated SWE is constantly about 10% lower than the observed, despite the two uppermost elevation bands, which are fine modelled. At Figure 3c and Figure 3d it can be seen, that the elevation band at 2700 to 2800 m is in a good agreement and again the upper ones are overestimated and the lower ones are underestimated by the simulation. This result is again due to the problem of vertical snow redistribution.

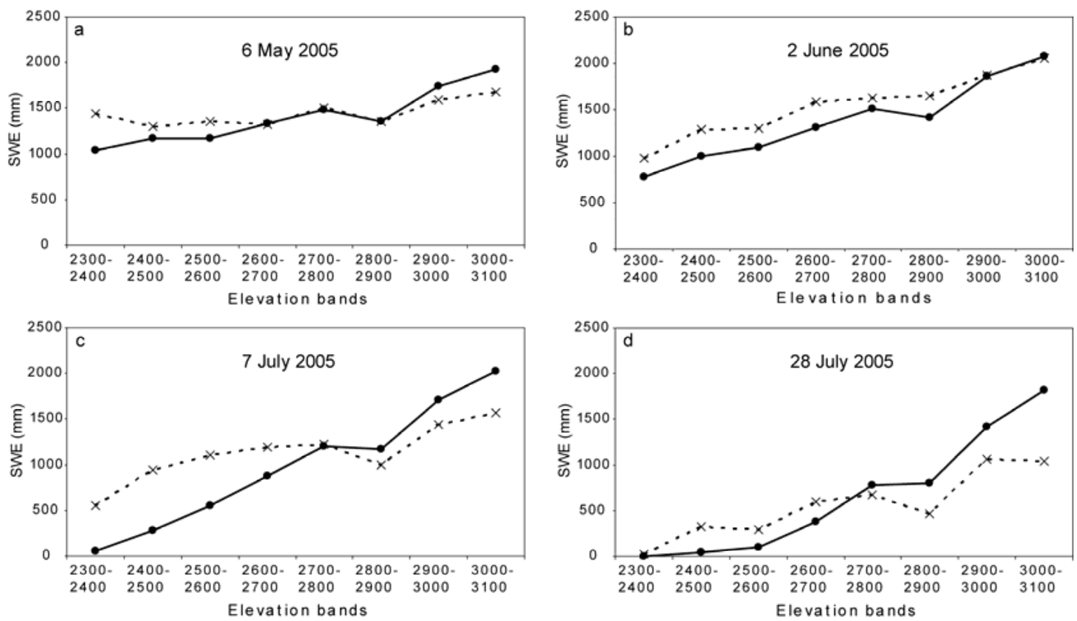

Figure 3. Simulated SWE (solid line, dots) vs. observed SWE (dashed line, x) averaged over 100 m elevation bands at four different points in time.

Figure 8b shows the observed daily snow depth at station 5 (Figure 1) and Figure 8c shows the simulated SWE averaged over the entire catchment area. The correlation coefficient calculated for the ascending phase is about $r^2=0.91$, for the descending $r^2=0.99$, and for the entire period $r^2=0.92$. We imply that the good correlation at the descending phase is due to a quite homogeneous snow density and quite similar snow melt processes over the entire catchment area. The ascending phase of the observed snow depth measurement (Figure 8b) shows typical settling effects of the snowpack, which can not be simulated by models without physically based assumptions for the snowpack modelling (Lehning et al., 2006).

Snow cover patterns

An ASTER (L1B) image of good quality has been available for 29 July 2005. The image has been classified (unpublished data from Vollmann, 2006) to generate a map of snow cover patterns. Figure 4 shows the comparison of the observed and simulated snow cover map. The lower parts of the catchment area are simulated as nearly snow free. The observation shows a more complex structure of the snow line retreat, but the simulated snow cover pattern is in a good agreement with the observed pattern. Inadequacies arise from processes not included in the model such as redistribution of snow by wind and avalanches (Blöschl et al., 1991; Lehning et al., 2000; Doorschot et al., 2001). At such small scale and with the adoption of such a high spatial resolution we can see the role of snow redistribution and understand how distributed models have to be improved to account for such processes.

Runoff simulations

For the 2005 melt season (calibration period) discharge data have been available for the period of 9 July–30 September (Figure 5).

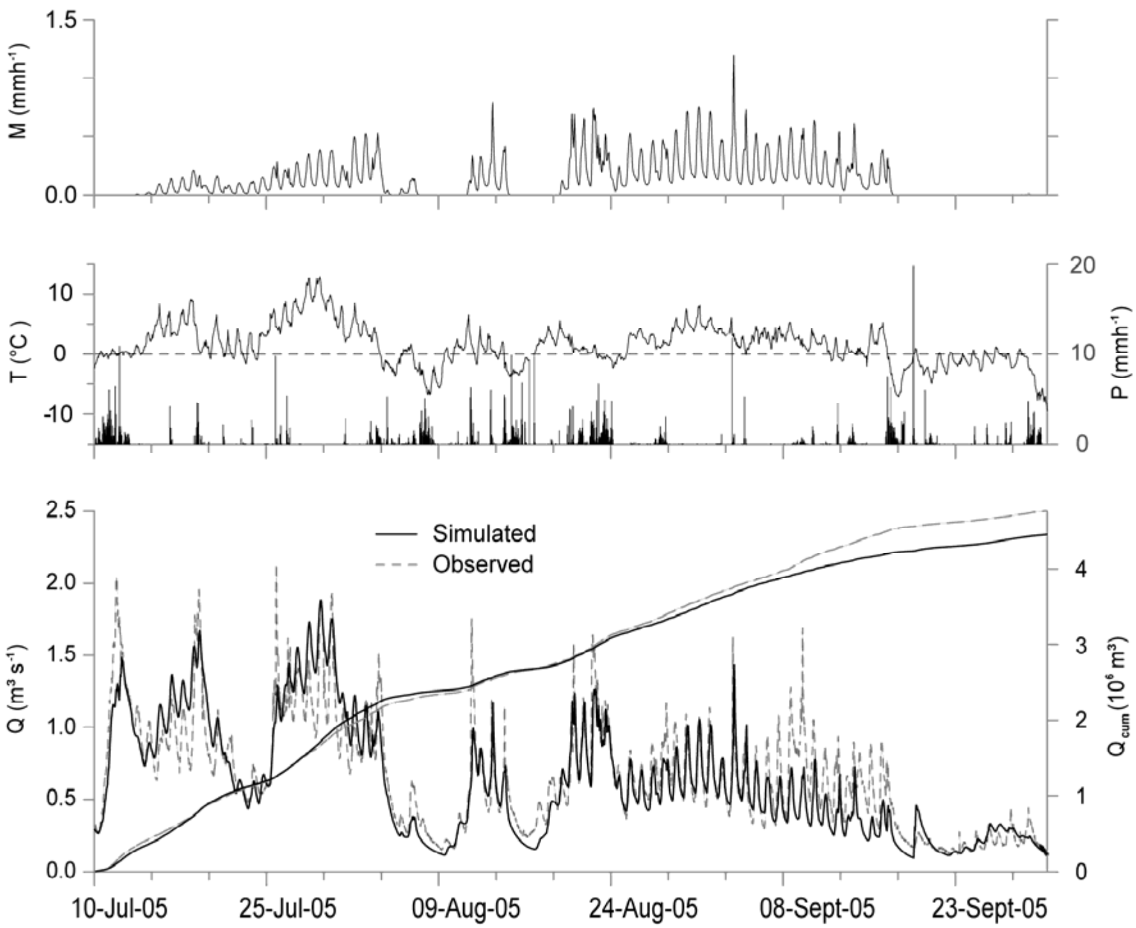

Figure 5. Simulated icemelt averaged over the catchment area, M (mm h^{-1}), hourly data of air temperature, T (°C), and precipitation P (mm h^{-1}) at Hoher Sonnblick observatory, and observed and simulated discharge Q (m^3 s^{-1}) at the catchment outlet of Goldbergkees. The increasing lines at the bottom plot indicate the cumulated discharge Q_{cum} (10^6 m^3) over the period of the discharge observations from 10 July to 30 September 2005.

The beginning of the observations shows rain-induced discharge peaks. Typical diurnal variations of the observed runoff, induced by icemelt are seen in the period from end of August until mid of September. The performance of the simulation has been employed according to the efficiency criterion R_{NS}^2 (Nash and Sutcliffe, 1970), defined as:

$$R_{NS}^{\ 2} = 1 - \frac{\sum_{i=1}^{n}(Q_{obs} - Q_{sim})^2}{\sum_{i=1}^{n}(Q_{obs} - \overline{Q_{obs}})^2} \tag{2}$$

where Q is the hourly value of the catchment runoff ($m^3\ s^{-1}$) and the subscripts obs and sim refer to the observed and simulated runoff. The bar refers to the mean of the observed runoff and n is the number of time-steps for which R_{NS}^2 is calculated. The final model performance accounts for $R_{NS}^2 = 0.77$. The scatter plot in Figure 6 shows the comparison of observed and simulated runoffs. It is seen, that low flow and mean flow conditions are good represented but that there are some higher values of discharges below the 45° line which have not been simulated. Higher discharges are cushioned through the quite high value of the snow melt storage time (25 h), since rainfall on the snow surface has to go through this storage. The lowering of the snow melt storage time would effect into a steep recession curve (e.g. recession between 4th and 5th of August in Figure 2) and on the other hand the lifting of peak discharges is quite low. Hence, the simulated runoff hydrograph shown in Figure 5 is the result of an optimization. The main nature of the observed hydrograph with respect to the diurnal and seasonal fluctuations through the superposition of melting processes are very good represented by the simulation.

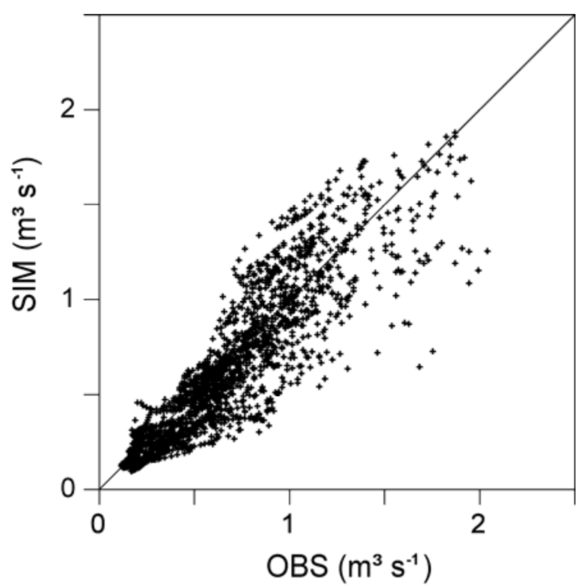

Figure 6. Scatter plot of the observed vs. simulated hourly discharge for the period from 10 July to 30 September 2005.

Looking at the entire simulation period of 2004/2005 (Figure 8, d) it is seen that there has been a time span of about five month with no flow. The earliest runoff processes of the melt season started at the beginning of May. During the period from May to July total discharge is mainly formed by snowmelt (see Figure 8, d and Figure 9). Peak discharges occur during June and July, where all components contributing to runoff, despite icemelt, reach their maximum.

For the verification season 2003/2004 the model has been run using the same set of parameters as shown in Table 1. Solid precipitation has been corrected by plus 18% like in the calibration period 2004/2005. The model performance, employed according to the efficiency criterion following Nash and Sutcliffe (1970), has been calculated for $R_{NS}^2 = 0.60$. Figure 7 presents the model results in detail. The hydrologic response of the Goldbergkees catchment has been different from the year 2004/2005 presented before, but the processes of snow- and icemelt are well simulated. A slightly overestimation of the simulated cumulated runoff can be seen. During

2003/2004 period only the meteorological input data of the observatory at Hoher Sonnblick (Figure 1, Nr. 1) has been available for simulations. Hence, there is a lack of input data for the interpolation and regionalisation of meteorological variables, which results in a lower model performance. Nevertheless this shows that the calibrated model is able to simulate different climatic conditions independently from additional validation data and re-calibration of model parameters.

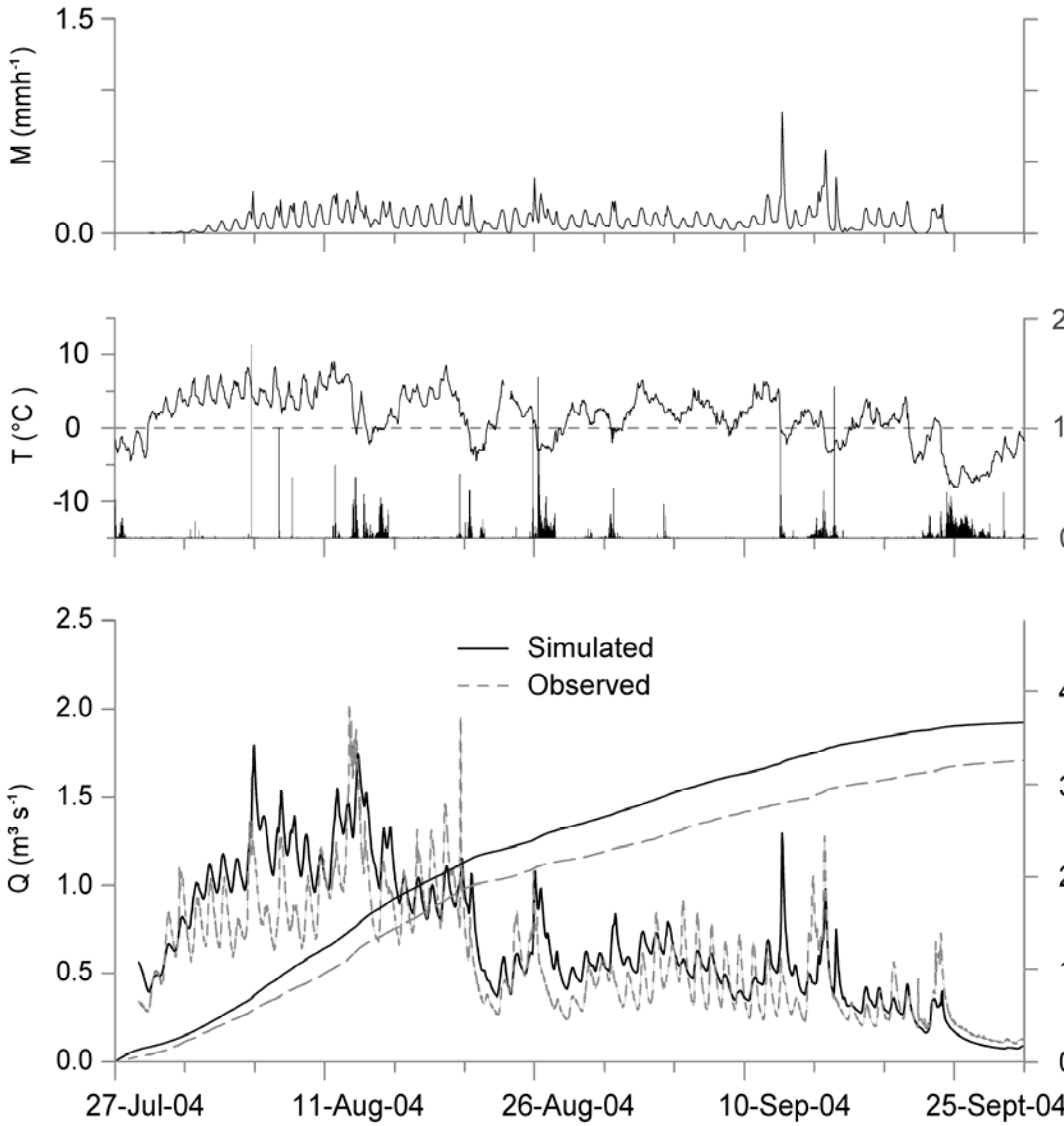

Figure 7. Simulated icemelt averaged over the catchment area, M (mm h^{-1}), hourly data of air temperature, T (°C), and precipitation P (mm h^{-1}) at Hoher Sonnblick observatory, and observed and simulated discharge Q (m^3 s^{-1}) at the catchment outlet of Goldbergkees. The increasing lines at the bottom plot indicate the cumulated discharge Q_{cum} (10^6 m^3) over the period of the discharge observations from 27 July to 30 September 2004.

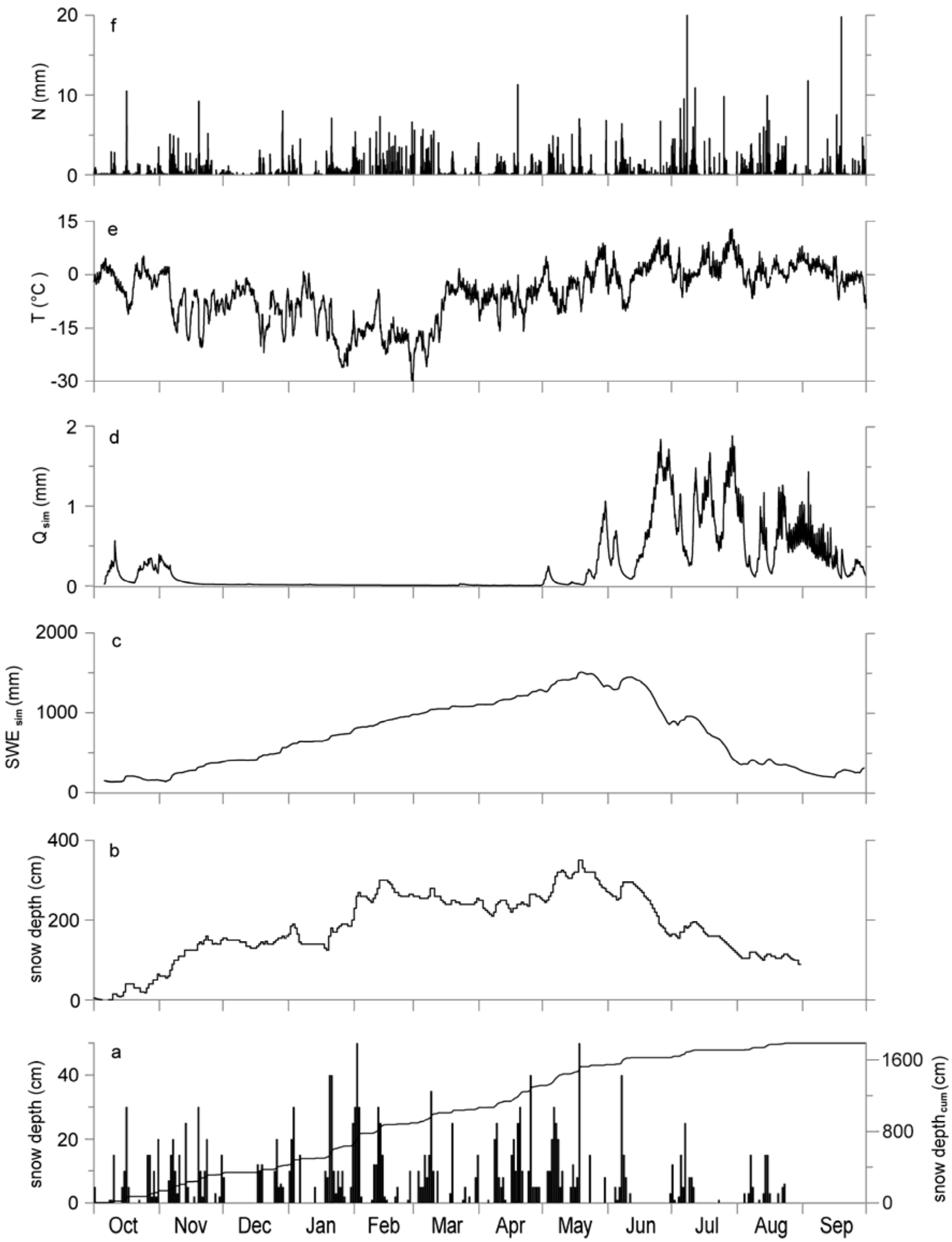

Figure 8. Main hydro-meteorological observations vs. simulated hourly discharge and daily output of the SWE storage. a: daily observed depths of fresh snow (cm) and cumulated depths of fresh snow (maximum at 1787 cm) over the period 1 October 2004 to 30 September 2005 at the automated ultrasonic station; b: daily measurements of the snow depth (cm) at the automated ultrasonic station; c: simulated SWE storage (mm); d: simulated hourly discharge ($m^3 s^{-1}$); e: hourly air temperature measurements (°C) at Hoher Sonnblick observatory; f: hourly precipitation (mm) at Hoher Sonnblick observatory.

Water balance

The water balance, as a final model result, states an additional possibility for the model validation. As the model generates output for all water balance components using easy balance equations the results of the hydrological year 2004/2005 (see Table 2) can be verified.

$$dS = (SWE_{end} - SWE_{begin}) - ICE_{melt}$$
$$dS = (309 - 152) - 277 = -120\ mm \qquad (3)$$

Table 2. Components of the annual water balance of Goldbergkees catchment for the hydrological year of 2004/2005

WB component	Values (mm)	Description
SWE_{begin}	152	SWE for model initialization at begin of October 2004
P_{adj}	2991	Adjusted precipitation over the catchment area
ETA	128	Real evapotranspiration
Q_{tot}	2956	Total runoff
$SNOW_{melt}$	2566	Total snowmelt
ICE_{melt}	277	Total icemelt
SWE_{end}	309	SWE left at the end of the period at end of September 2005

Equation 3 calculates the change of the main storages, where dS is the change of the storages over the entire simulation period. (definitions of symbols can be seen at Table 2)

$$WB = P_{adj} - Q_{tot} - ETA - dS$$
$$WB = 2991 - 2956 - 128 + 120 = 27\ mm \qquad (4)$$

Equation 4 evaluates the water balance, whereas WB is the annual water balance. The result of WB = 27 mm is explained by the difference of the base flow storage component at the simulation end minus the base flow storage value for the initialization at the beginning. Equation 5 shows the share of the components snow melt, icemelt and rainfall contributing to runoff.

$$Q = SNOW_{melt} + ICE_{melt} + RAIN_{direct}$$
$$=> RAIN = 2956 - 277 - 2566 = 113\ mm \qquad (5)$$

$RAIN_{direct}$ indicates the share of the total runoff which has been induced by effective rainfall, directly routed to discharge. Liquid precipitation ($RAIN_{direct}$) accounts for 3.8%, icemelt (ICE) accounts for 9.4%, and snowmelt (SNOW) accounts for 86.8%. The value for liquid precipitation seems to be underestimated, because snowmelt has a very high value. Snow melt is defined as the snow which is melted by the energy affecting the snow surface, whereas melted snow does not have to be routed directly to discharge.

The simulated snow accumulation reached its maximum at 20 May 2005 at 1507 mm (Figure 8, c), compared to SWE field measurements at 6 May 2005 showing a value of about 1391 mm. The monthly water balance is presented in Figure 9. Icemelt starts in July and typically has its maximum in August. Glacier melt was also simulated for November 2004, because of quite high temperatures at that time. Using field measurements of the ice ablation stakes during the hydrological year of 2004/2005, 510 mm of ice loss are calculated over the glacierized area (unpublished data from Schöner et al., 2006). The simulated ice loss accounts for 277 mm over the catchment area, which would be 502 mm assigned to the glacierized area. This very good agreement between simulated and observed icemelt is due to a reliable estimation of all modelled components. Evaporation accounted for 128 mm for the entire simulated year and is mainly affected by low temperatures at this alpine site.

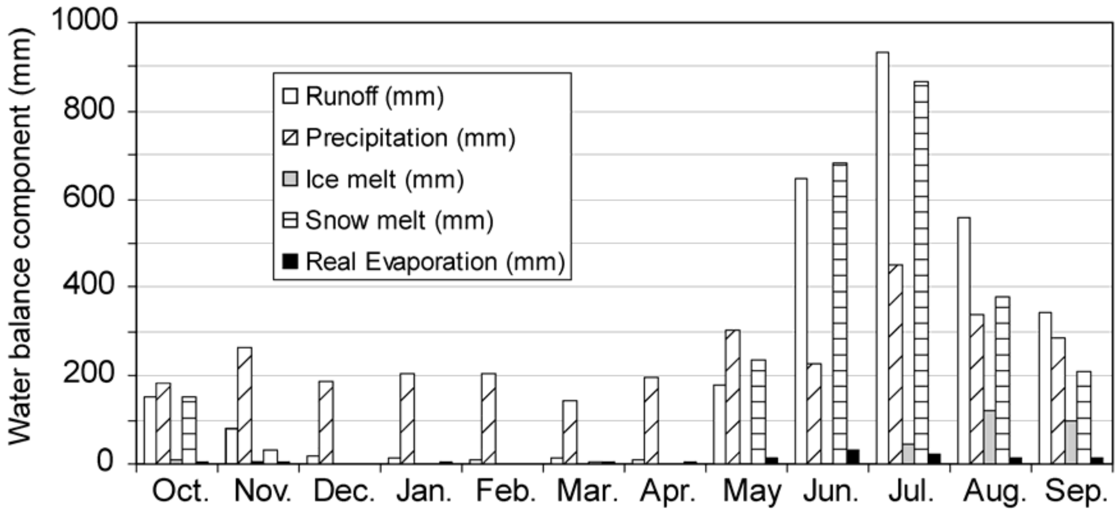

Figure 9. Monthly simulated balance of runoff (mm), precipitation (mm), icemelt (mm), snow melt (mm), and real evaporation (mm) averaged over the catchment area over the period October 2004 to September 2005.

The observed ice loss for the verification period of 2003/2004 accounted for 197 mm averaged over the glacierized area and the snow accumulation measured at the beginning of May 2004 accounted for 1744 mm (unpublished data from Schöner et al., 2006). The simulation results for the verification period accounted for 275 mm ice loss averaged over the glacier and 1690 mm of SWE calculated for the beginning of May. This means a slightly overestimation of the ice loss and a slightly underestimation of the snow accumulation . Once more we can show the quality of the stabile multi-validation approach used for the 2004/2005 period.

CONCLUSIONS AND OUTLOOK

The PREVAH model shows the ability to model the waterbalance as well as the discharge hydrograph of the high elevated Goldbergkees watershed. Melt processes have been simulated accurately in different temporal scales: the simulated diurnal variations of runoff matched the runoff observations during melt season and the seasonal balance is in a good agreement with the observed mass balance data. This paper has shown the need of various observed data like discharge hydrographs, distributed snow water equivalent and ice ablation data to guarantee a stabile cross-validation of simulation results (Verbunt et al. 2003). The model results concerning runoff relied on the input of precipitation and air temperature, all the other input has been necessary for the evaporation simulations. Hence, there should be a quite small operating expense for data acquisition for melt modelling, despite all the problems and uncertainties occurring during precipitation and air temperature measurements (Sevruk, 1986, 1989). The watershed of Goldbergkees has demonstrated its great advantage of having a meteorological observatory on site and long term and detailed mass balance measurements (Auer et al., 2002). The availability of spatial dense meteorological data of good quality at this isolated location is a unique feature and an advantage of the study region. Main efforts for the preparation of simulations have been due to the acquisitions of validating data, with respect to logistic manner, mountainous risks and strictly weather depending planning of field investigations.

As PREVAH does not include the redistribution of snow by wind or avalanches the spatial distribution of the SWE cannot be matched perfectly, but the mean values of the modelled SWE are identical to measured catchment means of the SWE. Hence, it seems that the main part of the drifted snow originates from the simulated watershed and remains inside. An additional conceptual module for the snow redistribution by wind and avalanches (Hartmann et al., 1999) should be applied to the model to satisfy these claims. It seems to be obvious, that only in a very good observed catchment area reliable simulation results of high quality can be obtained.

ACKNOWLEDGEMENTS

This ongoing research was supported by a grant from the Austrian Academy of Sciences under the project SNOWTRANS HOE29, part of the IHP PUB (International Hydrological Program, Prediction in Ungauged Basins). Many thanks to Markus Vollmann for the classification of the ASTER image. The authors are grateful to all the students, colleagues and friends who helped to carry out the exhausting field work.

REFERENCES

Arnold N., Richards K., Willis I., Sharp M. 1998. Initial results from a semi-distributed, physically based model of glacier hydrology. Hydrological Processes **12**: 191–219.

Arnold N.S., Willis I. C., Sharp M., Richards K.S., Lawson W. 1996. `A distributed surface energy balance model for a small valley glacier. I. Development and testing for the Haut Glacier d'Arolla, Valais, Switzerland', Journal of Glaciology, **42**: 77–89.

Auer I., Böhm R., Leymüller M., Schöner W., Kaiser A., Scheifinger H., Langer M., Scheider St., Häberli Ch. 2002. Das Klima des Sonnblicks. Klimaatlas und Klimatographie der GAW Station Sonnblick einschließlich der umgebenden Gebirgsregion. Österreichische Beiträge zu Meteorologie und Geophysik. Heft **28**. Zentralanstalt für Meteorologie und Geodynamik, Wien. ISSN 1016–6254.

Badoux A. 1999. Untersuchung zur flächendifferenzierten Modellierung von Abfluss und Schmelze in teilvergletscherten Einzugsgebieten. Diploma thesis at the Geographical Institute of ETH, Zürich.

Blöschl G., Kirnbauer R., Jansa J., Kraus K., Kuschnig D., Gutknecht D., Reszler C. 2002. Using remote sensing methods for calibrating and verifying a spatially distributed snow model. Österreichische Wasser- und Abfallwirtschaft (ÖWW) **54**: 16 pp.

Blöschl G., Kirnbauer R., Gutknecht D. 1991. Distributed Snowmelt Simulations in an Alpine Catchment, 1, Model Evaluation on the Basis of Snow Cover Patterns. Water Resources Research, **27**(12), 3171–3179.

Collins D.N., 1982. Water storage in Alpine glaciers. Hydrological Aspects of Alpine and High Mountain Areas (Proceedings of the Exeter Symposium, July 1982) IAHS Publ, no **138**: 113–122.

Doorschot J., Raderschall N., Lehning M. 2001. Measurements and one-dimensional model calculations of snow transport over a mountain ridge. Annals of Glaciology, **32**: 153–158.

Elder K., Rosenthal W., Davis R.E. 1998. Estimating the spatial distribution of snow water equivalence in a montane watershed. Hydrological Processes **12**: 1793–1808.

Finsterwalder S., Schunk H. 1887. Der Suldenferner. Zeitschrift des Deutschen und Oesterreichischen Alpenvereins **18**: 72–89.

Gurtz J., Zappa M., Jasper K., Lang H., Verbunt M., Badoux A., Vitvar T. 2003. A Comparative Study in Modelling Runoff and its Components in Two Mountainous Catchments. Hydrological Processes **17**: 297–311. DOI: 10.1002/hyp.1125

Güntner A., Uhlenbrook S., Seibert J., Leibundgut C. 1999. Multi-criterial validation of TOPMODEL in a mountainous catchment. Hydrological Processes 13: 1603–1620.

Hartman M.D., Baron J.S., Lammers R.B., Cline D.W., Band L.E., Liston G.E. Tague C. 1999. Simulations of snow distribution and hydrology in a mountain basin. Water Resources Research, **35**(5): 1587–1603.

Hock R. 1999. A distributed temperature-index ice- and snowmelt model including potential direct solar radiation. Journal of Glaciology **45(149)**: 101–111.

Hock R., Holmgren B. 2005. A distributed surface energy-balance model for complex topography and its application to Storglaciären, Sweden. Journal of Glaciology **51(172)**: 25–36.

Hoinkes H. 1970. Methoden und Möglichkeiten von Massenhaushaltsstudien auf Gletschern. Ergebnisse der Meßreihe Hintereisferner (Ötztaler Alpen) 1953–1968. Zeitschrift für Gletscherkunde und Glazialgeologie, **6**, 37 – 90.

Hynek B., Schöner W. 2004. Massenhaushalt 2002/2003 der Gletscher in der Goldberggruppe. **101–102.** Jahresbericht des Sonnblick-Vereines: 1–15. Eigenverlag der Zentralanstalt für Meteorologie und Geodynamik, Wien.

Kaser G., Fountain A., Jansson P. 2003. A manual for monitoring the mass balance of mountain glaciers. IHP-VI, Technical Documents in Hydrology **No. 59**, UNESCO, Paris, 2003.

Kirnbauer R, Blöschl G, Gutknecht D. 1994. Entering the Era of Distributed Snow Models. Nordic Hydrology **25**: 1–24.

Klok E.J., Jasper K., Roelofsma K.P., Gurtz J., Badoux A. 2001. Distributed hydrological modelling of a heavily glaciated Alpine river basin. Hydrological Sciences Journal—Journal Des Sciences Hydrologiques **46**: 553–570.

Lang H., Braun L. 1990. On the Information content of air Temperature in the Context of Snow Melt Estimation. In: Hydrology of Mountainous Areas, L. Molar (Ed.). IAHS Publ. no. **190**: 347–354.

Lehning M., Voelksch I., Gustafsson D., Nguyen T.A., Stähli M., Zappa M. 2006. Influence of snow, forest, soil and local meteorological forcing on mountain catchment hydrology. Hydrological Processes, in press: DOI: 10.1002/hyp.6204.

Lehning M., Doorschot J., Bartelt P. 2000. A snowdrift index based on SNOWPACK model calculations. In Annals of Glaciology, **31**: 382–386.

Marks D., Domingo J., Susong D., Link T., Garen D. 1999. A spatially distributed energy balance snowmelt model for application in mountain basins. Hydrological Processes **13**:1935–1959.

Nash J.E., Sutcliffe J.V. 1970. River flow forecasting through conceptual models (1), a discussion of principles. Journal of Hydrology **10** (3): 282–290.

Ohmura A. 2001. Physical Basis for the Temperature-Based Melt-Index Method. Journal of Applied Meteorology **40**, No. 4: 753–761. DOI: 10.1175/1520-0450(2001)040<0753:PBFTTB>2.0.CO;2

Østrem G., Brugman M. 1991. Glacier mass-balance measurements—A manual for field and office work: Environment Canada, National Hydrology Research Institute Science Report **No. 4**, and Norwegian Water Resources and Energy Administration, 224 p.

Pellicciotti F., Brock B., Strasser U., Burlando P., Funk M. Corripio J. 2005. An enhanced temperature-index glacier melt model including the shortwave radiation balance: development and testing for Haut Glacier d'Arolla, Switzerland. Journal of Glaciology **51(175)**: 573–587.

Ross B.B., Contractor D.N., Shanholtz V.O. 1979. A Finite Element Model Of Overland And Channel Flow For Assessing The Hydrologic Impact Of Landuse Change. Journal of Hydrology **41**: 1–30.

Schaefli B., Hingray B., Niggli M., Musy A. 2005. A conceptual glacio-hydrological model for high mountainous catchments, Hydrology and Earth System Sciences Discussions **2**: 73–117.

Sevruk B. (ed.) 1986. Correction of Precipitation Measurements. ETH/IASH/WMO Workshop on the Correction of Precipitation Measurements. Zürich, April 1–3, 1985, Zuercher Geographische Schriften, Heft **23**.

Sevruk B. (ed.) 1989. Precipitation Measurement. Proc. of the WMO/IASH/ETH Workshop on Precipitation Measurement. St. Moritz, December 3–7, 1989, WMO Instruments and Observing Methods Rep., No. 48, WMO/TD-No. 328, 199–204, 1989, Geneva.

Singh P., Bengtsson L. 2005. Impact of warmer climate on melt and evaporation for the rainfed, snowfed and glacierfed basins in the Himalayan region. Journal of Hydrology **300**: 140–154. DOI: 10.1016/j.hydrol.2004.06.005

Verbunt M., Gurtz J., Jasper K., Lang H., Warmerdam P., Zappa M. 2003. The hydrological role of snow and glaciers in alpine river basins and their distributed modelling. Journal of Hydrology **282**: 36–55. DOI: 10.1016/S0022-1694(03)00251-8

Zappa M., Pos F., Strasser U., Gurtz J. 2003. Seasonal water balance of an alpine catchment as evaluated by different methods for spatially distributed snow melt modelling. Nordic Hydrology **34(3)**: 179–202

Zappa M, Badoux A., Gurtz J. 2000. The application of a complex distributed hydrological model in a highly glaciated alpine river catchment, in Limnological Reports, Horvatic J. (Editor), 33rd Conference of International Association for Danube Research, Osijek, Croatia, 3–9 Sept. 2000, Vol. **33**: 23–28.